RESEARCH ARTICLE

Structural Coupling between RNA Polymerase Composition and DNA Supercoiling in Coordinating Transcription: a Global Role for the Omega Subunit?

Marcel Geertz,[a*] Andrew Travers,[b,c] Sanja Mehandziska,[a] Patrick Sobetzko,[a] Sarath Chandra Janga,[b*] Nobuo Shimamoto,[d] and Georgi Muskhelishvili[a]

Jacobs University, Bremen, Germany[a]; MRC Laboratory of Molecular Biology, Cambridge, United Kingdom[b]; Fondation Pierre-Gilles de Gennes pour la Recherche, c/o LBPA, École Normale Supérieure de Cachan, Cachan, France[c]; and National Institute of Genetics, Mishima, Japan[d]

*Present addresses: Marcel Geertz, Université de Genève, Département de Biologie Moleculaire, 30 quai Ernest-Ansermet, CH-1211 Geneva 4, Switzerland; Sarath Chandra Janga, Institute for Genomic Biology, University of Illinois at Urbana-Champaign, Champaign, Illinois, USA.

ABSTRACT In growing bacterial cells, the global reorganization of transcription is associated with alterations of RNA polymerase composition and the superhelical density of the DNA. However, the existence of any regulatory device coordinating these changes remains elusive. Here we show that in an exponentially growing *Escherichia coli rpoZ* mutant lacking the polymerase ω subunit, the impact of the Eσ^{38} holoenzyme on transcription is enhanced in parallel with overall DNA relaxation. Conversely, overproduction of σ^{70} in an *rpoZ* mutant increases both overall DNA supercoiling and the transcription of genes utilizing high negative superhelicity. We further show that transcription driven by the Eσ^{38} and Eσ^{70} holoenzymes from cognate promoters induces distinct superhelical densities of plasmid DNA *in vivo*. We thus demonstrate a tight coupling between polymerase holoenzyme composition and the supercoiling regimen of genomic transcription. Accordingly, we identify functional clusters of genes with distinct σ factor and supercoiling preferences arranging alternative transcription programs sustaining bacterial exponential growth. We propose that structural coupling between DNA topology and holoenzyme composition provides a basic regulatory device for coordinating genome-wide transcription during bacterial growth and adaptation.

IMPORTANCE Understanding the mechanisms of coordinated gene expression is pivotal for developing knowledge-based approaches to manipulating bacterial physiology, which is a problem of central importance for applications of biotechnology and medicine. This study explores the relationships between variations in the composition of the transcription machinery and chromosomal DNA topology and suggests a tight interdependence of these two variables as the major coordinating principle of gene regulation. The proposed structural coupling between the transcription machinery and DNA topology has evolutionary implications and suggests a new methodology for studying concerted alterations of gene expression during normal and pathogenic growth both in bacteria and in higher organisms.

Address correspondence to Georgi Muskhelishvili, g.muskhelishvili@jacobs-university.de.

During bacterial growth, changes in environmental conditions induce coordinated alterations of genomic expression. In the classical model organism *Escherichia coli*, such coordinated changes are especially conspicuous in genome-wide transcriptional responses to experimentally induced alterations of chromosomal DNA topology (1–3). Topological alterations of DNA are normally associated with growth transitions (4), but the regulatory device that coordinates the instant response of global transcription to variations in DNA supercoiling remains unspecified. The process of transcription by RNA polymerase (RNAP) is intimately linked to the overall structure and superhelicity of the DNA in the bacterial nucleoid context (5), and there is ample evidence that DNA supercoiling is under the control of a homeostatic network comprising DNA topoisomerases, abundant nucleoid-associated proteins (NAPs), and the components of the transcription machinery (6–18). Since regulation of supercoiling necessitates the sensing of topological transitions in DNA, the networked genes themselves explicitly respond to changes in overall superhelicity (2, 3, 12, 19–21).

The cross talk between NAPs and DNA topoisomerases has been implicated in partitioning of the constrained and free DNA supercoils, generating topological domains and spatial transcription patterns in the genome (1, 3, 18, 22–28). Therefore, mutations of NAPs can alter both the overall superhelicity and the transcriptional response to variations in supercoiling (3, 29–31). Accordingly, under conditions of DNA relaxation and high negative supercoiling, NAPs organize distinct chromosomal domains with coherently expressed genes (18, 32). This type of transcriptional regulation depends on the available supercoil energy and is therefore dubbed a continuous or "analog" type of control, as

opposed to the "digital" control exerted by specific binding of dedicated transcription factors (TFs) targeting a few high-affinity DNA sites in the gene promoter regions (32). The major impact of analog control on cellular physiology is evident from observations that the transcription of both the genes mediating adaptation to stress and the genes of central metabolic pathways of assimilation and dissimilation is coordinated by their distinct responses to DNA superhelicity (3, 33–36). Perhaps unsurprisingly, the biosynthetic genes are preferentially transcribed under conditions of high negative superhelicity, whereas transcription of catabolic genes involved in energy production is activated under conditions of DNA relaxation (3). Importantly, the introduction of negative supercoils into the DNA by the E. coli DNA gyrase depends on the ATP/ADP ratio, such that the overall superhelicity correlates with the phosphorylation potential in the cell (37–39). The availability and utilization of supercoil energy will therefore vary with the physiological state, supporting the notion of tight coupling between cellular metabolism and chromatin architecture (3, 14, 18, 36, 40).

The E. coli RNAP, acting as a unique transcribing machine, requires its composition to be adapted during bacterial growth to genome-wide changes in chromatin architecture. Genomic transcription sustaining fast cellular growth is normally associated with high levels of negative superhelicity and is driven predominantly by RNAP containing the major σ^{70} subunit encoded by the rpoD gene, whereas overall DNA relaxation on the transition to stationary phase (4) is correlated with enhanced utilization of the alternative σ^{38} subunit encoded by the rpoS gene (41, 42). In fast-growing cells under conditions of high phosphorylation potential, the σ^{38} protein interacts with a phosphorylated form of the RssB protein and is subsequently degraded by the ClpXP protease (43), such that the maximal gyrase activity and σ^{38} availability appear anticorrelated. Accordingly, studies on isolated promoters showed that the Eσ^{70} and Eσ^{38} holoenzymes favor highly supercoiled and more relaxed DNA for transcription, respectively (44, 45). Whether the distinct topological preferences of the Eσ^{70} and Eσ^{38} holoenzymes play a role in determining the supercoiling regimen of genomic transcription remains unclear. Yet, this question is of central importance for understanding the coordinated transcriptional responses observed during bacterial growth transitions and adaptation. On the assumption that the major metabolic pathways are coordinated by their distinct responses to supercoiling (3, 36), a shift in RNAP holoenzyme composition could provide a straightforward mechanism for reorganizing metabolism by switching the supercoiling regimen of genomic transcription.

In this study, we addressed this question by investigating the influence of the compositional alterations of RNAP on the overall DNA superhelicity and the supercoiling preferences of transcription in growing E. coli cells. We identified distinct transcription programs utilizing alternative clusters of σ factor- and supercoiling-dependent genes to sustain bacterial exponential growth and propose a role for the ω subunit of RNAP in optimizing the transcription of highly negatively supercoiled DNA.

RESULTS

Deletion of ω alters the σ^{70} content of RNAP. We explored the relationships between RNAP composition and DNA topology using the E. coli CF1943 wild-type strain and an isogenic CF2790 rpoZ mutant lacking the RNAP ω subunit, in which our previous studies revealed topological alterations of DNA (M.G. and G.M.,
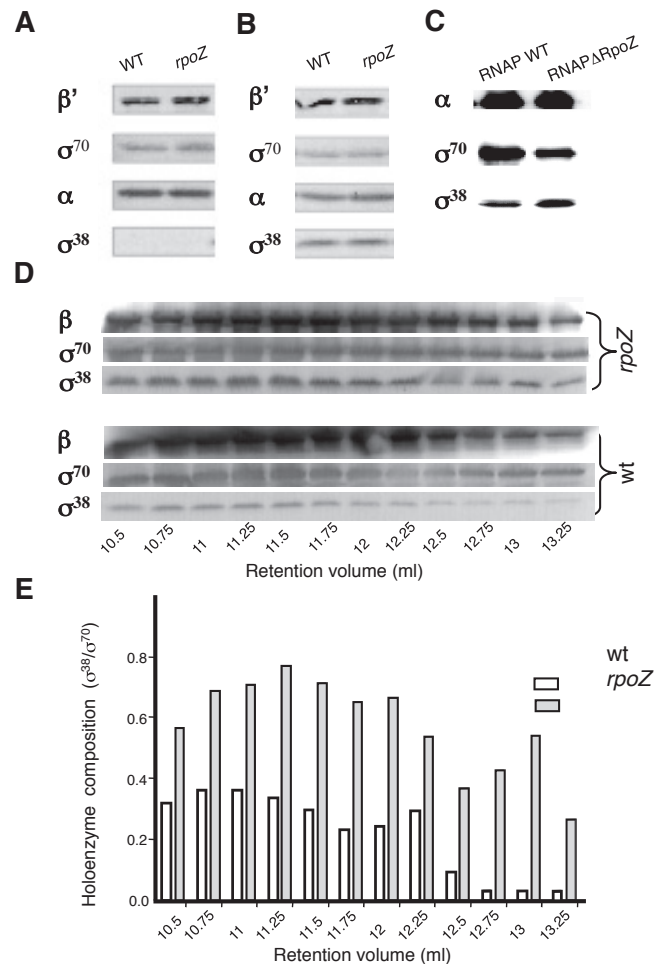

FIG 1 Deletion of ω leads to depletion of σ^{70} and enrichment for σ^{38} in the RNAP holoenzyme. (A) Western blot analyses of the crude cellular extracts of exponentially growing CF1943 wild-type (WT) and isogenic CF2790 rpoZ mutant cells using antibodies against the β', σ^{70}, σ^{38}, and α subunits. (B) Western blot analyses of the crude cellular extracts of stationary-phase (overnight) cultures of CF1943 and CF2790 rpoZ mutant cells using antibodies against the β', σ^{70}, σ^{38}, and α subunits. (C) Western blot analyses of purified RNAP preparations isolated from exponentially growing CF1943 wild-type and CF2790 rpoZ mutant cells using antibodies against the α, σ^{70}, and σ^{38} subunits. (D) Fractionation of CF1943 wild-type and CF2790 rpoZ mutant whole-cell extracts (harvested at an OD of 1; see Fig. 2A) by size exclusion chromatography. Fractions containing the RNAP holoenzyme were subjected to Western analysis using antibodies against β, σ^{70}, and σ^{38}. (E) Quantification of the σ^{38}/σ^{70} ratios in the RNAP holoenzyme fractions of wild-type and rpoZ mutant cells using Western blot assays as shown in panel D. The values represent averages from two independent fractionation experiments.

data not shown). The doubling times during growth at 37°C in rich 2× YT medium were 25.7 min for the wild type and 26.5 min for the mutant. RNAP subunit composition was monitored by Western analyses of whole-cell extracts and purified holoenzyme preparations isolated from exponentially growing cells. In cellular extracts, no significant differences in σ^{38} and σ^{70} subunit content were observed (Fig. 1A and B). However, in purified RNAP preparations isolated from the rpoZ mutant, the σ^{70} subunit was noticeably depleted whereas the σ^{38} subunit appeared slightly enriched (Fig. 1C). Since analyses of both whole-cell extracts and purified preparations may not faithfully reflect the RNAP compo-
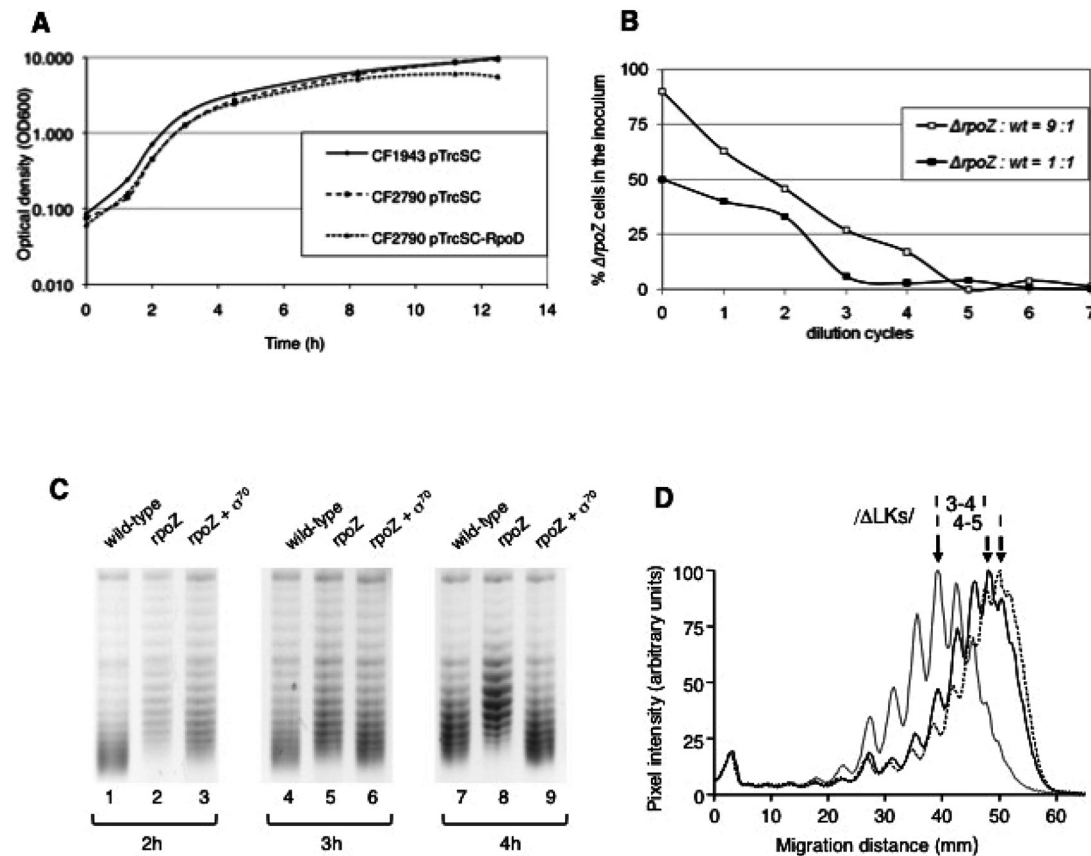
FIG 2 Effect of changing RNAP composition on DNA topology. (A) Growth curves of CF1943 wild-type cells, CF2790 *rpoZ* mutant cells mock transfected with pTrcSC, and CF2790 *rpoZ* mutant cells with the pTrcSC-RpoD plasmid overproducing σ^{70} after inoculation into fresh 2× YT medium. (B) Growing CF1943 cells have a selective advantage over CF2790 *rpoZ* mutant cells. Wild-type (*wt*) and mutant (chloramphenicol-resistant) cells were combined at either a 1:1 (black squares) or a 9:1 (open squares) proportion and diluted 1:10,000 into fresh medium. After 12 h of growth, two equal aliquots were plated on a selective medium containing chloramphenicol and on a nonselective solid medium. This procedure was repeated several times, and after each dilution cycle (abscissa), the percentage of chloramphenicol-resistant survivors on the selector plates was scored. The ordinate shows the percentage of chloramphenicol-resistant colonies. (C) High-resolution agarose gel electrophoresis of plasmid pACYC184 isolated from exponentially growing wild-type and *rpoZ* mutant cells with and without overproduction of σ^{70}. Tracks 1 to 3, 4 to 6, and 7 to 9 correspond to 2 h, 3 h (mid-log phase), and 4 h (late-log phase) after inoculation, respectively. The genetic backgrounds of the host and the σ^{70} overproducer are indicated above the tracks. More negatively supercoiled topoisomers migrate faster in this gel. (D) Digital scans of topoisomer distributions (centers indicated by arrows) of three plasmid populations isolated 4 h after inoculation as shown in tracks 7 to 9 of panel C. Black line, wild type; grey line, *rpoZ* mutant; dotted line, *rpoZ* mutant overproducing σ^{70}. Differences in the equilibrium distribution of the topoisomers (/ΔLks/) between the wild type and the *rpoZ* mutant ($|\Delta Lk| = 3$ to 4) and between the *rpoZ* mutants with and without σ^{70} overproduction ($|\Delta Lk| = 4$ to 5) are indicated.

sition found *in vivo*, we fractionated cell extracts by size exclusion chromatography to quantify the relative amounts of the σ^{38} and σ^{70} subunits in eluted holoenzyme fractions. Determinations of σ^{38}/σ^{70} ratios clearly demonstrated enrichment for the Eσ^{38} holoenzyme in the cellular extracts of *rpoZ* mutant cells (Fig. 1D and E). These results are in keeping with the previously proposed "latching" effect of the ω subunit on Eσ^{70} holoenzyme assembly (46, 47) and suggest a shift of the Eσ^{38}/Eσ^{70} holoenzyme balance in the *rpoZ* mutant.

RNAP composition impacts overall DNA topology *in vivo*. We next assessed the influence of *rpoZ* mutation on DNA topology using plasmid pACYC184 as a reporter of overall DNA superhelical density in wild-type and mutant cells, which grew at similar rates under our experimental conditions (Fig. 2A). Nevertheless, growing wild-type cells have a clear selective advantage over the *rpoZ* mutant (Fig. 2B). Since we failed to overproduce the RpoZ protein from an expression vector in the *rpoZ* mutant (data not shown), to counterbalance the increased Eσ^{38}/Eσ^{70} ratio observed

in the *rpoZ* mutant, we overproduced σ^{70} from the episomal *rpoD* gene (pTrcSC-RpoD; see Materials and Methods) and monitored its influence on the topology of plasmid pACYC184. High-resolution gel electrophoresis analyses of the topoisomer distributions of the plasmids isolated at intervals after the inoculation of cells into fresh medium demonstrated a global relaxation of pACYC184 DNA in *rpoZ* mutant cells (linking deficit [$|\Delta Lk|$] = 3 to 4), whereas overproduction of σ^{70} in this mutant increased the average negative superhelicity to levels comparable to wild-type levels during the mid- to late-exponential phase ($|\Delta Lk| = 4$ to 5; Fig. 2C and D). The same procedure did not affect the plasmid topology in wild-type cells (data not shown). We infer that an increased Eσ^{38}/Eσ^{70} ratio is associated with global relaxation of DNA in the exponentially growing *rpoZ* mutant, whereas overproduction of σ^{70} restores the high levels of negative superhelicity.

Deletion of ω alters the σ factor selectivity of promoter recognition. To compare the effective impacts of the Eσ^{70} and Eσ^{38} holoenzymes in the wild-type and *rpoZ* mutant backgrounds, we
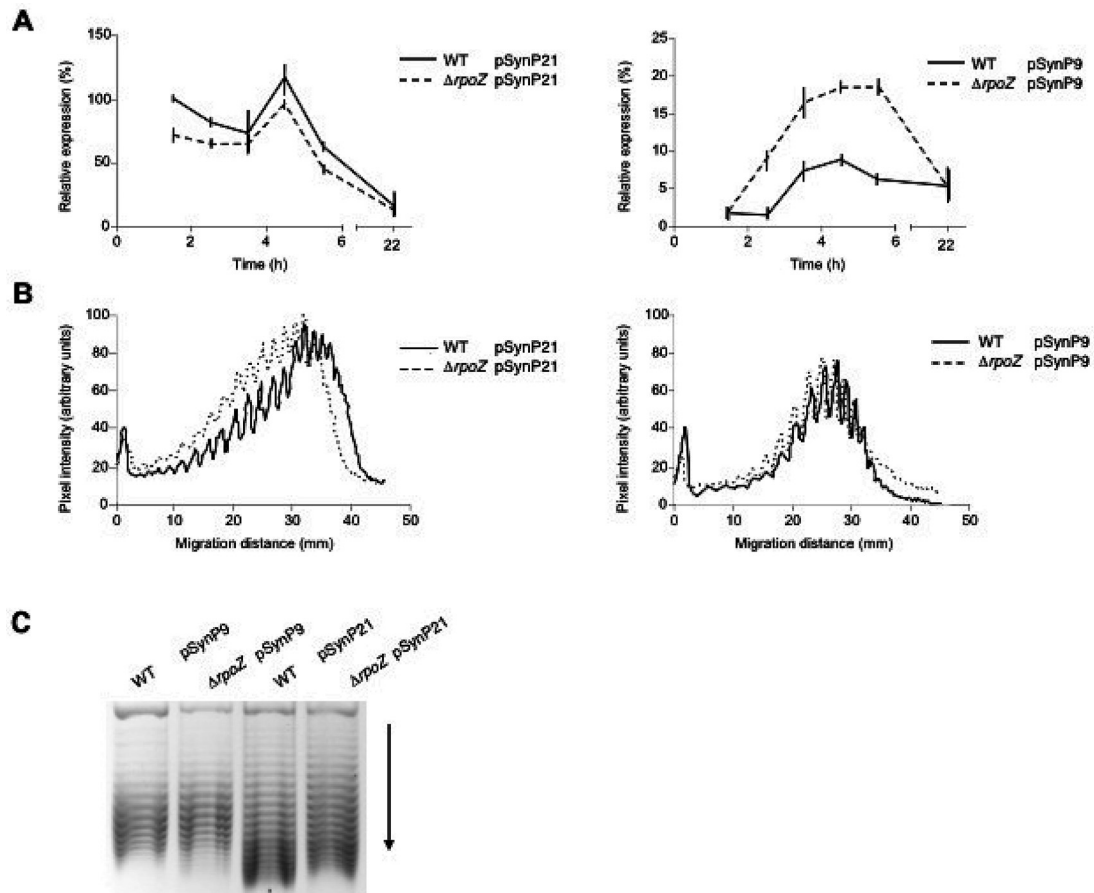
FIG 3 Deletion of ω enhances the Eσ^{38} selectivity of transcription *in vivo*. (A) Relative expression of pSynP21 (left panel) and pSynP9 (right panel) determined by real-time PCR at intervals after inoculation of wild-type (WT) and *rpoZ* mutant cells in fresh medium. (B) Digital scans of topoisomer distributions of pSynP21 (left panel) and pSynP9 (right panel) plasmid populations isolated from exponentially growing wild-type and *rpoZ* mutant cells. (C) High-resolution agarose gel electrophoresis of pSynP21 and pSynP9 plasmid preparations isolated from exponentially growing wild-type and *rpoZ* mutant cells. More negatively supercoiled topoisomers migrate faster in this gel. The direction of migration in the gel is indicated by the arrow.

employed pSynP21 and pSynP9 constructs carrying synthetic promoters selectively recognized by the Eσ^{70} and Eσ^{38} holoenzymes, respectively (48; see Materials and Methods). The strains were transformed with synthetic promoter constructs, and the amount of specific transcripts produced during bacterial growth was quantified by real-time PCR (see Materials and Methods). Comparisons of the Eσ^{70}-dependent SynP21 promoter activities in wild-type and *rpoZ* mutant cells demonstrated that the transcription rates varied with growth, being slightly lower in the mutant at most time points (Fig. 3A, left panel). In contrast, the Eσ^{38}-dependent SynP9 promoter was both activated earlier and transcribed at a significantly higher rate in the *rpoZ* mutant (Fig. 3A, right panel), fully consistent with an increased proportion of the Eσ^{38} holoenzyme observed in fractionated extracts of mutant cells (Fig. 1). A similar bias was observed when we compared the Eσ^{70}-dependent *fis* and Eσ^{38}-dependent *dps* promoter activities in wild-type and *rpoZ* mutant cells (see Fig. S1 in the supplemental material). Furthermore, when we compared the topologies of the pSynP21 and pSynP9 plasmids isolated from exponentially growing wild-type and *rpoZ* mutant cells, we found that the pSynP9 plasmid demonstrated lower negative superhelical density than pSynP21 in both strains (Fig. 3B and C). Since pSynP9 is prefer-

entially transcribed by the Eσ^{38} holoenzyme, this finding strongly suggests that the global relaxation of DNA observed in the *rpoZ* mutant during exponential growth is due to an increased impact of the Eσ^{38} holoenzyme, whereas increased negative superhelicity on the overproduction of σ^{70} reflects an enhanced effective impact of Eσ^{70} overriding the DNA relaxation phenotype.

The σ factor-dependent reorganization of transcription. Since the DNA relaxation phenotype of the *rpoZ* mutant was apparently complemented by the overproduction of σ^{70}, we asked whether this overproduction also induced a transcription program for exponential growth similar to that of the wild type. For this purpose, we used microarray analyses to compare the DNA transcript profiles of wild-type and *rpoZ* mutant cells on the one hand and *rpoZ* mutant cells with and without overproduction of σ^{70} on the other. Two separate sets of the differential transcripts thus obtained were together subjected to average-linkage cluster analysis (see Materials and Methods) identifying coherently expressed genes. The gene transcripts showing high log ratios (upregulated) in *rpoZ* mutant backgrounds from both experiments formed together four clusters (clusters 3 to 6 in Fig. 4), whereas the genes showing high log ratios in the σ^{70}-complemented *rpoZ* mutant and in wild-type cells formed two clusters (respectively, clus-
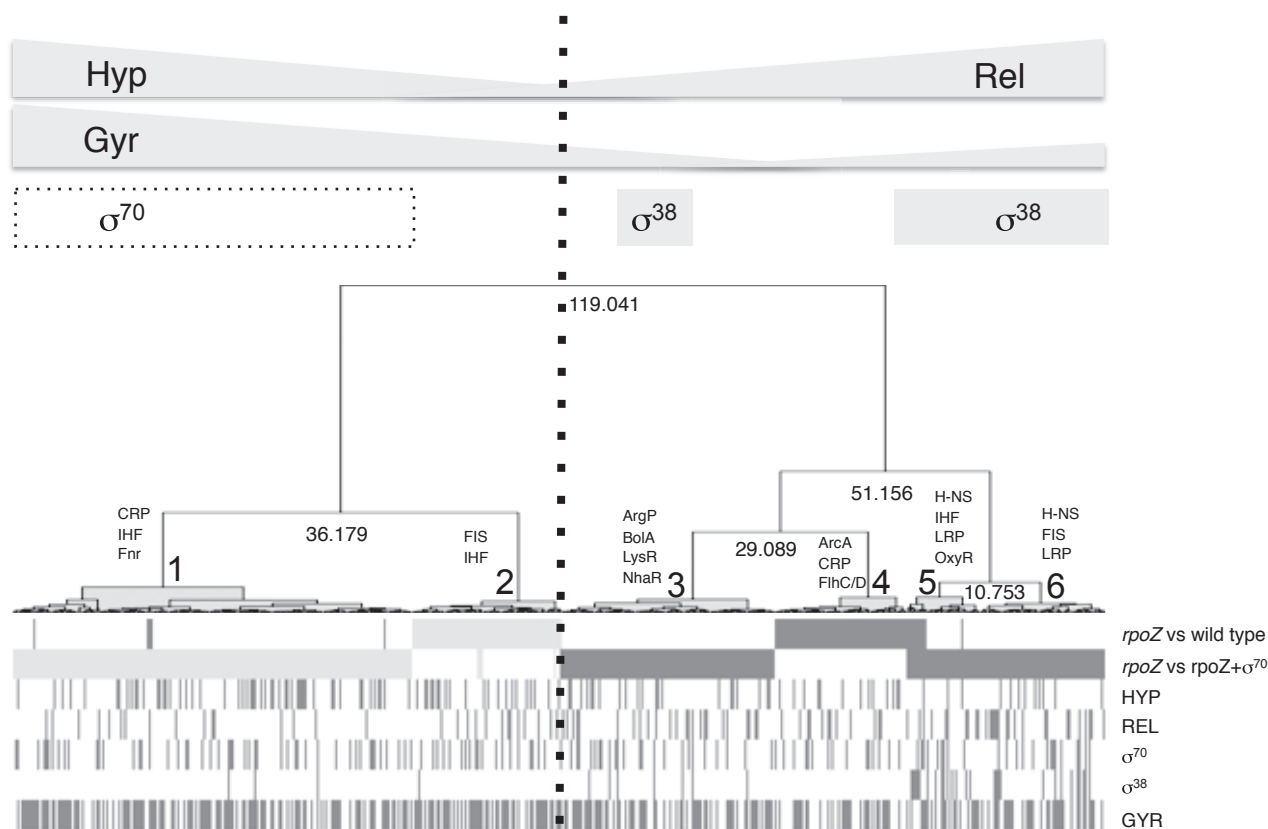
FIG 4 Cluster analysis of transcript profiles. Clusters shown as light and dark grey bars are numbered 1 to 6. Cluster 2 corresponds to genes upregulated in wild-type cells compared to *rpoZ* mutant cluster 4. Cluster 1 corresponds to genes upregulated in the *rpoZ* mutant overproducing σ^{70} from pTrcSC-RpoD (indicated by the dashed rectangle) compared to the *rpoZ* mutant mock transfected with pTrcSC (clusters 3, 5, and 6). The distributions of *hyp* and *rel* genes, gyrase binding sites, and σ factor dependences are shown as barcodes at the bottom. Coefficients of correlation between clusters and the main TFs impacting the clusters are indicated.

ters 1 and 2 in Fig. 4; for full clustered gene lists, see Table S1 in the supplemental material). In these six clusters, we analyzed the σ factor selectivity of the gene promoters using the RegulonDB database (49) and calculated Z scores to evaluate the significance of the observed distributions (Table 1). Interestingly, clusters 1 and 2 were not conspicuously enriched for σ^{70}-dependent genes, perhaps because the annotation of the σ^{70} dependence of promoters is far from complete. However, in these two clusters, only a small number of σ^{38}-dependent genes was found, suggesting that transcription is programmed predominantly by Eσ^{70} polymerase. In contrast, the four clusters comprising the transcripts upregulated in the *rpoZ* mutant background contained many σ^{38}-dependent

genes (especially clusters 5 and 6; Fig. 4; Table 1), fully consistent with the increased impact of Eσ^{38}-programmed transcription observed in *rpoZ* mutant cells.

Supercoiling preferences of gene clusters. Previous studies identified about 300 genes distinctly responding to DNA relaxation (2), whereas direct transcriptome comparisons of E. *coli* cells grown under conditions of DNA relaxation or hypernegative DNA supercoiling, including mutant strains lacking the NAPs, allowed an almost 10-fold increase in the number of identified supercoiling-sensitive genes (3, 36). The latter data set, successfully used in previous studies to link the supercoiling response to both genomic expression patterns and cellular metabolism (3, 32,

TABLE 1 Composition of the identified clusters of sigma factors and supercoiling sensitivity

Cluster	Size (no. of genes)	No. of ORFs (Z score)[a]				
		hyp	*rel*	σ^{70}	σ^{38}	*gyr*
1	197	53 (2.50)	16 (−3.80)	49 (−0.33)	3 (−1.20)	123 (16.00)
2	74	21 (1.90)	13 (−0.24)	20 (0.23)	1 (−0.79)	51 (11.00)
3	105	21 (0.06)	24 (1.10)	23 (−0.93)	7 (2.30)	61 (11.00)
4	65	13 (−0.04)	12 (−0.04)	15 (−0.50)	0 (−1.40)	30 (5.80)
5	36	3 (−1.70)	10 (1.40)	9 (−0.12)	14 (13.00)	20 (5.80)
6	62	9 (−1.00)	19 (2.40)	14 (−0.61)	13 (8.40)	33 (7.30)

[a]Within each cluster, the numbers of known σ^{38} and σ^{70} transcribed ORFs, the supercoiling sensitivities of the ORFs, and the gyrase binding sites within the ORFs were determined. Corresponding Z scores were calculated for each analyzed parameter by comparison of detected values with appropriate null models.

36), was employed to determine the supercoiling preferences of the six identified clusters. We found that clusters 1 and 2, respectively corresponding to the wild type and the σ^{70}-complemented *rpoZ* mutant, were enriched for hypernegative (*hyp*) genes (Fig. 4; Table 1). Conversely, Eσ^{38}-controlled clusters 3, 5, and 6 from the *rpoZ* mutant background were enriched for genes responding to DNA relaxation (*rel*). These findings are fully consistent with the background-dependent differences in the topology of isolated plasmids (Fig. 2). Since DNA gyrase is the major enzyme introducing negative supercoils into DNA, we have also analyzed the frequency distributions of gyrase binding sites using the available library of sequences identified in the E. coli genome (1). We found that, compared to clusters 5 and 6, cluster 1 was noticeably enriched for gyrase binding sites (Table 1). Taken together, these results suggest that, by and large, a combination of two variables—σ factor selectivity and the supercoiling dependence of genes— underlies the organization of clusters.

Properties of the impacting transcriptional regulators. We next analyzed the transcriptional regulators constraining the effective transcriptional regulatory networks (32) in each cluster (see Table S2 in the supplemental material; Fig. 4). We found that although the gene clusters share the NAPs, each cluster is impacted by a unique combination of NAPs and dedicated TFs. Notably, the regulatory impacts of FIS, IHF, and CRP were observed in clusters with opposite supercoiling and σ factor preferences, whereas the impacts of H–NS and LRP were conspicuous only in Eσ^{38}-controlled clusters 5 and 6. Furthermore, in clusters 1 and 2, associated with high negative superhelicity, we observed the impacts of several regulators (AgaR, CyrR, ExuR, MalT, NarL, NarP, and SrlR) which respond to conditions of high negative supercoiling or are repressed by relaxation of DNA; conversely, the regulators impacting clusters 3 to 6 associated with DNA relaxation in the *rpoZ* mutant (BolA, DnaA, Fur, GadE, GadW, GatR, IscR, LacI, NhaR, OxyR, and TrpR) were found to respond to DNA relaxation (2, 3; M.G. and G.M., unpublished data). Finally, when we analyzed the distributions of annotated Eσ^{70} and Eσ^{38} promoters among the genes of the impacting regulators themselves, we again found that the regulators of clusters 3 to 6 pooled together were enriched for σ^{38}-dependent genes in comparison with regulators of pooled clusters 1 and 2, where we did not find any significant bias (see Table S3 in the supplemental material).

Couplon matrix analysis. To verify the increased impact of the Eσ^{38} holoenzyme in the *rpoZ* mutant by an independent method, we used couplon matrix analysis, which enables the measurement of significant changes both in the regulons corresponding to individual regulators (be it a NAP or a σ factor) and in couplons— subsets of regulons jointly regulated by distinct combinations of σ factors and NAPs (40). Couplon analysis was carried out with the same two sets of differential transcripts obtained from comparisons of (i) wild-type and *rpoZ* mutant cells and (ii) *rpoZ* mutant cells with and without overproduction of σ^{70}. In the first pool, the genes that were upregulated in the wild-type background (cluster 2) did not reveal any significant changes, whereas analysis of genes upregulated in the *rpoZ* mutant background (cluster 4) demonstrated changes in the σ^{38} regulon (Fig. 5A and B). Similar analyses of the second set of differential transcripts demonstrated significant changes in the CRP/σ^{70} couplon, as well as the CRP and Fnr regulons in the σ^{70}-complemented *rpoZ* mutant background (cluster 1, Fig. 5C). In contrast, the genes upregulated in the *rpoZ* mutant background without σ^{70} overproduction (clusters 3, 5,

and 6) revealed significant changes in all of the NAP/σ^{38} couplons, as well as in the entire σ^{38} regulon (Fig. 5D). Thus, the couplon matrix analysis also indicates an increased impact of the Eσ^{38} holoenzyme in the *rpoZ* mutant background in both sets of differential transcripts. Taken together, our observations suggest that in wild-type and *rpoZ* mutant cells, the compositionally different RNAP holoenzymes utilize distinct combinations of NAPs and supercoiling regimens for the assembly of alternative transcription programs sustaining exponential bacterial growth.

DISCUSSION

In this study, we show that during the exponential growth of the *rpoZ* mutant lacking the RNAP ω subunit, Eσ^{38}-programmed transcription is increased in concert with an overall reduction in negative superhelicity and a preferential utilization of genes associated with DNA relaxation. Conversely, overproduction of σ^{70} in this mutant complements the DNA relaxation phenotype and leads to the preferential transcription of genes associated with high negative superhelicity. While this suggests a tight coupling between holoenzyme composition and DNA topology, a noteworthy difficulty in assessing the impact of holoenzyme composition on DNA supercoiling arises from the peculiarity of the transcription process, which itself, independent of the molecular constitution and source of the holoenzyme, affects supercoil dynamics and the overall shape of the DNA (50, 51). It is assumed that the supercoil dynamics of the genomic DNA depend on the strength of transcription (26). Consistently, we observe a correlation between the rate of transcription (compare the relative expression levels on the ordinates of graphs in the right and left panels of Fig. 3A) and overall superhelical density of isolated pSynP21 and pSynP9 plasmids (Fig. 3B and C). However, we note that the transcription of plasmids pSynP21 and pSynP9 is preferentially driven by the Eσ^{70} and Eσ^{38} holoenzymes, respectively, and that only negligible topological change is associated with substantially increased pSynP9 construct transcription in the *rpoZ* mutant compared to that in the wild-type strain (compare Fig. 3A and B, right panels). We propose, therefore, that the molecular composition of the holoenzyme is the primary determinant of both the strength of transcription and the associated DNA superhelicity *in vivo*. Early studies suggested that mutations of RNAP can alter global DNA supercoiling (52, 53), and several lines of evidence are consistent with a direct impact of the molecular composition of RNAP on overall DNA topology. It was observed that changes in RNAP composition affect not only the specificity of promoter sequence recognition (54) but also the preference for the binding of upstream sequences (48). Furthermore, holoenzyme composition was found to determine the extent of the DNA wrapped in the initial complex (55). In addition, compositional changes in RNAP could modulate the interactions with secondary channel regulators, DNA topoisomerases, and DNA architectural factors (27, 56–58), thus transmitting the compositional change to DNA superhelicity. Other conceivable possibilities for composition-dependent effects of RNAP on DNA topology include altered propensities to generate R loops or form transcription foci (18, 59, 60).

A global role for ω? Our data implicate ω in the optimization of the Eσ^{70}-programmed transcription of highly negatively supercoiled DNA during exponential growth. How can loss of the RNAP ω subunit lead to reorganization of transcription? The *rpoZ* gene is transcribed during exponential growth (M.G. and G.M., unpublished), but it is not clear whether every polymerase mole-
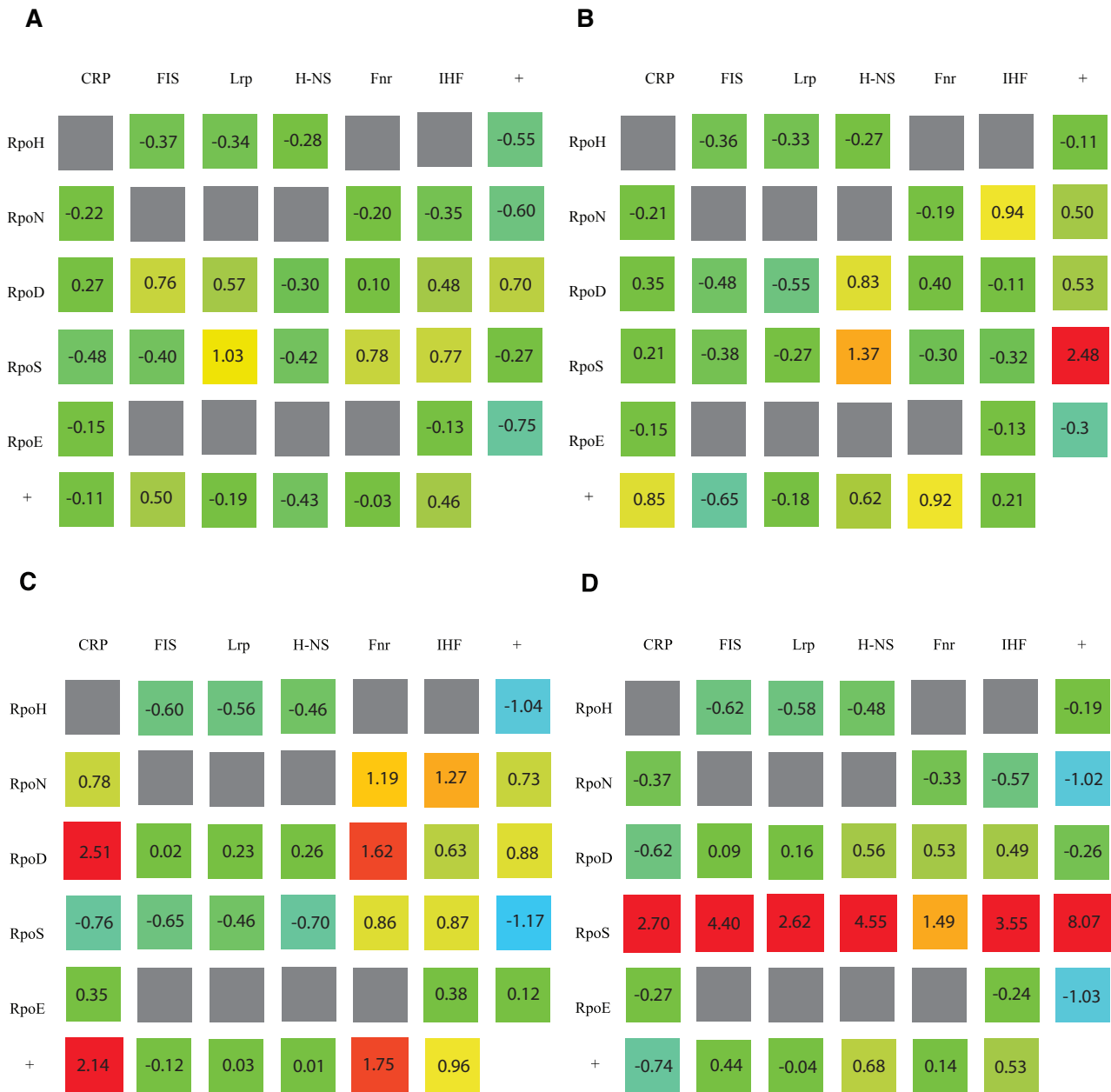
FIG 5 Couplon analyses of transcript profiles. The couplon matrix is organized by orthogonally intersecting regulons (derived from the RegulonDB E. *coli* K-12 transcriptional network) of the NAPs and RNAP σ factors indicated on the horizontal and vertical axes, respectively. Each square at an intersection thus defines a distinct couplon coordinated by two coupled regulators (40). In each panel, the last rows and columns indicated by plus signs represent the entire regulons. Rainbow colors indicate significantly increased (red) or decreased (blue) numbers of genes in the effective profile set compared to 10,000 equal-sized random input sets. Corresponding Z scores (values inside squares) are indicated. (A) Couplon matrix of upregulated genes in the wild-type background (cluster 2). (B) Couplon matrix of upregulated genes in the *rpoZ* mutant background (cluster 4). (C) Couplon matrix of upregulated genes in the *rpoZ* mutant background with σ⁷⁰ overproduction from pTrcSC-RpoD (cluster 1). (D) Couplon matrix of upregulated genes in the *rpoZ* mutant background plus mock transfection with pTrcSC (i.e., without σ⁷⁰ overproduction; clusters 3, 5, and 6).

cule is associated with ω (61). Yet, our stoichiometry determinations (see Fig. S2 in the supplemental material) suggest that during exponential growth there is at least one copy of ω per RNAP molecule. Therefore, a simple hypothesis is that the phenotype of the *rpoZ* mutant is dependent on structural changes in the RNAP holoenzyme lacking the latching effect of ω (46, 47).

Since the phenotypic effects of the loss of ω can be suppressed by overproduction of σ^{70}, it is conceivable that ω modulates the relative affinities of σ^{38} and σ^{70} for the core polymerase. The σ factor competition is subject to complex regulation involving the "alarmone" ppGpp (62), which represses the "stringent" promoters utilizing Eσ^{70} (e.g., stable RNA promoters) and activates the Eσ^{38}-dependent promoters and also those Eσ^{70}-dependent promoters involved in the response to stress (63). However, in the *rpoZ* mutant, the "stringent response" is not impaired (64) nor is stable RNA transcription diminished (65), although in the ab-

sence of ω, the altered sensitivity to ppGpp could be masked by the secondary channel regulator DksA (66). Notably, DksA is not only implicated in the balance of secondary channel regulators compensating for certain effects of ppGpp (67, 68) but also modulates the topological barriers to supercoil diffusion (27). Another relevant regulator would be the Crl protein facilitating $E\sigma^{38}$ holoenzyme assembly (69, 70), but we did not find changes in either *dksA* or *crl* expression in our transcriptome studies (see Table S1 in the supplemental material). The possibility of a direct effect of ω on σ factor competition thus remains an attractive hypothesis to be elucidated.

Alternative programs for exponential growth. Our observation of alternative ways of organizing transcription programs sustaining fast exponential growth—one utilizing mainly $E\sigma^{70}$ and the other utilizing both the $E\sigma^{70}$ and $E\sigma^{38}$ holoenzymes—reveals a new flexibility of genetic regulation and is in keeping with the notion that σ^{38} is acting as a second vegetative σ factor under nonoptimal growth conditions (71). These alternative growth programs employ functional gene clusters with distinct σ factor and DNA topology preferences (Fig. 4). In $E\sigma^{70}$-dependent cluster 1, enriched for *hyp* genes, we also calculated the highest Z score for associated gyrase binding sites, whereas clusters 5 and 6 showed both increased $E\sigma^{38}$ selectivity and an increased preference for *rel* genes (Table 1). Clusters 3 and 4 appear less clearly defined. Perhaps unsurprisingly, clusters preferring different holoenzymes nevertheless share the impacting global regulators—the NAPs (Fig. 4; see Table S2 in the supplemental material). Yet, for each cluster, the constellations of regulators are different, suggesting substantial combinatorial flexibility in optimizing transcription. More specifically, the impact of H–NS and LRP, known as modulators of $E\sigma^{38}$ selectivity (53, 72), was detected in $E\sigma^{38}$-dependent clusters 5 and 6 (see Table S2), whereas the impact of FIS was observed in two clusters (2 and 5) with opposite σ factor-supercoiling couplings. This is consistent with buffering effects of FIS on $E\sigma^{70}$-dependent promoters requiring high negative superhelicity (e.g., stable RNA promoters) that are rescued by FIS on DNA relaxation and also with comodulation of gene expression by FIS and σ^{38} (73, 74). Similarly, the impact of CRP observed in distinct clusters 1 and 4 is consistent with both the proposed cooperation between σ^{38} and CRP (42) and the existence of two promoters enabling *crp* transcription under different supercoiling regimens (20).

While the overproduction of σ^{70} in wild-type cells has no effect on holoenzyme composition (75), in the exponentially growing *rpoZ* mutant, the directional switch of the transcription program is especially conspicuous when cells with and without σ^{70} overproduction are compared. The significant changes in couplons observed in the *rpoZ* mutant under these conditions (Fig. 5D) suggest cross talk between $E\sigma^{38}$ and the NAPs on the relaxation of DNA. In keeping with this observation, in the *rpoB114* mutant containing the "stringent" RNAP holoenzyme with impaired sensitivity to ppGpp, increased production of IHF is associated with overall DNA relaxation (76; M.G. and G.M., unpublished). Importantly, despite overall DNA relaxation and increased $E\sigma^{38}$-programmed transcription, under our experimental conditions, wild-type and *rpoZ* mutant cells grew at comparable rates, such that a selective growth advantage of wild-type cells could be revealed only under conditions of direct competition (Fig. 2A and B). This suggests that sufficient $E\sigma^{70}$ is available in *rpoZ* mutant cells for stable RNA synthesis, as previously reported (65), and that reduced overall superhelicity *per se* does not necessarily pre-

clude efficient growth, as inferred also from the "experimental evolution" study of E. *coli* populations (77). Indeed, the phenotype of the *rpoZ* mutant does not resemble the phenotype induced by σ^{70} underproduction (78). However, overproduction of σ^{70} in this mutant represses the *uspB* and *uspF* genes, as well as other stress-related genes normally activated on the transition to stationary phase (see Table S1 in the supplemental material). This is in keeping with the recently proposed $E\sigma^{70}$-dependent shift in balance toward cellular growth at the expense of maintenance (75). Nevertheless, despite similar growth rates, the transcription profiles of exponentially growing wild-type and σ^{70}-complemented *rpoZ* mutant cells are substantially different, again consistent with remarkable flexibility of genetic regulation.

Coordination of genomic transcription. In order to coordinate genomic transcription with physiological demands, the RNAP holoenzyme has to both integrate the entire information processed by the homeostatic network and organize the environment in which it operates. Importantly, the expression of transcription machinery components of the network, including the *rpoD* gene, is strongly dependent on DNA superhelicity (2, 3), whereas we show here that RNAP composition can, in turn, determine the supercoiling regimen of genomic transcription. We thus reveal a relationship of interdependence which is pivotal for coordinating genomic transcription, as alterations of DNA topology and transcription machinery can be reciprocally transmitted (40). The identification of clusters of alternative σ factor- and supercoiling-dependent genes suggests a simple mechanism for rearranging metabolism by coupling the different holoenzyme forms with distinct structural dynamics of DNA at the genome-wide level. What is the structural basis of this coupling? Observed differences in cognate promoter sequence organization (54, 79), in preferences for distal and proximal half-sites of the UP elements (48), and in the propensity to wrap DNA (55) implicate the $E\sigma^{70}$ and $E\sigma^{38}$ holoenzymes in the recognition of different supercoil structures. By selecting distinct DNA geometries, these holoenzymes could determine the relative expression of abundant NAPs constraining different superhelical densities and thus optimize the σ factor selectivity of transcription (17, 44, 45, 72).

We propose that interdependent alterations of transcription machinery composition and DNA topology represent a basic regulatory device coordinating genome-wide transcription during bacterial growth and adaptation (Fig. 6). This necessarily raises the question of how tight this interdependence is. For example, overproduction of σ^{38} does not induce $E\sigma^{38}$-dependent *osmE* transcription until relaxation of the template DNA (45). This observation, together with our data presented in Fig. 1, suggests that it is the effective concentration of a particular holoenzyme that matters and not the cellular concentration of a σ factor *per se*. We believe that an exploration of structural coupling between the transcription machinery and chromosomal DNA topology has far-reaching evolutionary implications, providing a new methodology for studying the coordinating principles of gene regulation during normal and pathogenic growth in both bacterial and eukaryotic cells (80).

MATERIALS AND METHODS

Bacterial strains and plasmids. Isogenic E. *coli* K-12 strains CF1943 (wild type) and CF2790 (*rpoZ* mutant) (64) were used throughout this study. The σ^{70} protein was overproduced using pTrcSC-rpoD, a derivative of pTrc99A (81) harboring the *rpoD* gene and a pSC101 replication origin.
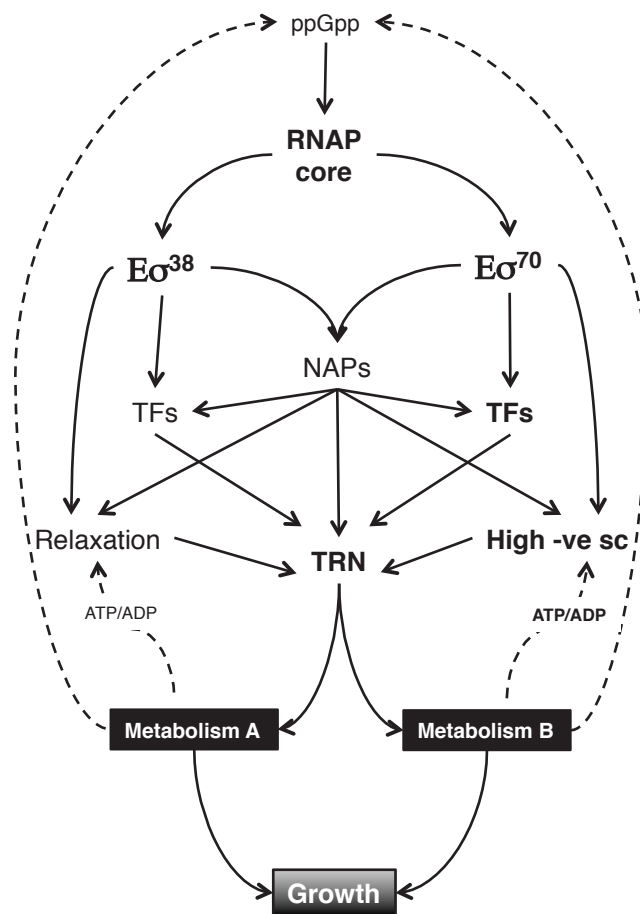
FIG 6 Coordination of transcription by structural coupling between the transcription machinery and DNA topology. In this model, a shift in the holoenzyme σ factor composition determines both the preferred superhelicity for transcription and the subsets of NAPs and dedicated TFs cooperating in the assembly of the transcription program. The subsets of NAPs, in turn, optimize the utilization of DNA superhelicity (3, 36), fine-tune TF selection, and also act themselves as hubs in the transcriptional regulatory network. In this way, distinct combinations of regulators coordinate genomic transcription with metabolism, thus sustaining alternative growth programs A and B. Metabolism feeds back into DNA topology and RNAP composition by determining the ATP/ADP ratios and ppGpp concentration and thus affecting gyrase activity (37–39) and σ factor competition (62, 63), respectively. As we show in this study, lack of ω leads to an increased impact of $E\sigma^{38}$-driven transcription, but the altered program nevertheless can support exponential bacterial growth. The regulatory effects of the anti-sigma factors and degrading proteases are omitted for clarity. For further details, see the text. -ve sc, negative superhelicity.

Synthetic promoter constructs pSynp21 and pSynp9 (kind gift of Regine Hengge, Freie Universität Berlin), are variants of pSynp213 derived from the core P_{tac} promoter and translationally fused to the *lacZ* gene (48).

The competition experiment between CF1943 and chloramphenicol-resistant CF2790 *rpoZ* mutant cells for the determination of a selective growth advantage was carried out as described by Schneider et al. (82). Briefly, overnight cell suspensions of the two strains after mixing at different ratios and subsequent growth for 12 h were diluted 1×10^{-6} before plating and the percentages of survivors on chloramphenicol plates were scored. The final concentration of chloramphenicol in the selective plates was 25 μg/ml. The cultures were again diluted 1:10,000 in fresh 2× YT medium and allowed to grow for a further 12 h. This procedure was repeated seven times.

Purification of RNAP. Bacterial cultures were grown under carefully controlled conditions in BIOSTAT Bplus (Sartorius AB, Göttingen, Ger-

many). The holoenzymes were purified from exponentially growing cells by high-performance liquid chromatography (82, 83). In brief, crude cell extract was loaded onto a HiPrep 16/10 heparin FF column (GE Healthcare, Munich, Germany). The collected peak fraction was reloaded onto a Mono Q 5/50 GL column (GE Healthcare, Munich, Germany) and polished using an Amicon Ultra-4 100K centrifugal filter (Millipore, Schwalbach, Germany).

Western analyses. Quantitative Western analyses (ECF kit; GE Healthcare, Munich, Germany) of crude cellular extracts and purified RNAP preparations were performed using mouse monoclonal antibodies raised against the β′, β, α, σ^{70}, and σ^{38} subunits (Neoclone, Madison, WI). Quantifications were carried out using a PhosphorImager.

Analysis of plasmid transcription. For quantifications of transcripts produced from the pSynp21 and pSynp9 plasmids, total RNA was extracted using the Qiagen RNeasy MinElute cleanup kit, followed by DNase I digestion using the Qiagen RNase-Free DNase set (Qiagen GmbH, Hilden, Germany). An additional DNase I treatment was performed using the Ambion RNase-free DNase I kit (Applied Biosystems, Foster City, CA). RNA concentrations were determined at 260 nm using a NanoDrop ND-1000 spectrophotometer, and transcripts were quantified by one-step real-time PCR using the Quanti-Tect SYBR green kit (Qiagen GmbH, Hilden, Germany) and an Mx3000P real-time cycler (Stratagene, La Jolla, CA).

The primers used for real-time PCR are as follows: pSyn_for, 5′ CCC TATTCAGCAATGCAACC 3′; pSyn_rev, 5′ GTAAAACGACGGGAGCA AGC 3′.

Fractionation of cellular extracts. Wild-type and *rpoZ* mutant cells were grown in 2× YT at 37°C to an optical density (OD) at 600 nm of 1. The cells were harvested, washed with phosphate-buffered saline, and resuspended in 5 ml of equilibration buffer (10 mM Tris-HCl [pH 7.8], 0.1 mM dithiothreitol, 0.1 mM EDTA, 200 mM NaCl). Cells were disrupted by sonication in the presence of protease inhibitor mix HP (Serva, Heidelberg, Germany) and 10 U/ml Benzonase (Sigma-Aldrich Chemie GmbH, Steinheim, Germany). After clearance of whole-cell extracts by centrifugation at 10,000 × g for 1 h at 4°C, a total of 3.5 mg of protein was applied to a size exclusion column (Superose 6 10/300; GE Healthcare) using an ÄKTA system (GE Healthcare). Elution with equilibration buffer was performed at the recommended flow rate of 0.5 ml/min at 4°C. Fractions of 250 μl were acetone precipitated, analyzed by 12% SDS-PAGE, and transferred onto a polyvinylidene difluoride membrane for Western analyses. Experiments were performed twice with reproducible results.

High-resolution gel electrophoresis. High-resolution gel electrophoresis of plasmids was carried out as described previously (21). The ImageQuant software was used to analyze topoisomer distributions and estimate the ΔLk value by the band-counting method (84).

DNA microarray analyses. All of the strains used for transcript profiling were grown in 2× YT medium at 37°C. DNA microarray experiments were performed using OciChip E. *coli* K-12 V2 arrays according to the OciChip application guide (Ocimum Biosolutions, Hyderabad, India) as previously described (3). In brief, for each comparison, two biological replicates with two technical replicates were performed, resulting in a total of 8 hybridizations. Scanned array images were analyzed using the TM4 software package (85). Spot intensities were quantified, and the quality of each spot was verified by calculating a quality control (QC) score depending on the signal-to-noise ratio for every channel and calculating *P* values for each channel (as a result of a *t* test comparing the spot pixel set and the surrounding background pixel set) using the Spotfinder software from The Institute for Genomic Research (TIGR). Data were normalized by locally weighted linear regression (86). A one-class *t* test (87) was applied to obtain differentially expressed genes within each data set (significance level, α < 0.05).

Cluster analysis of the transcript profiles. Ward's linkage cluster analysis based on a Euclidean distance matrix was applied to gene expression data sets. Within each cluster, σ^{70} and σ^{38} dependencies, TF-target gene (TG) relationships, and supercoiling sensitivities of transcript profiles were determined. While σ^{70} and σ^S dependencies and TF-TG rela-

tionships were derived from the RegulonDB database (49), supercoiling sensitivities were determined as described previously (3). A publicly available chromatin immunoprecipitation-chip data set was used and analyzed as described in the DNA microarray section to investigate open reading frames (ORFs) that show significant gyrase binding (1; Gene Expression Omnibus accession number GSE1735). Within each cluster, Z scores for σ dependencies, TF-TG relationships, supercoiling sensitivities, and gyrase binding were calculated from the mean and standard deviation of 10,000 runs of the corresponding null model (i.e., random sampling of $n_{\text{cluster size}}$ genes).

Couplon analyses. Couplon analyses were carried out using the coordination matrix and measuring couplon penetrance essentially as described in reference 40.

Microarray data accession number. The microarray data reported here have been submitted to the Array Express database and assigned accession number E-MEXP-942.

SUPPLEMENTAL MATERIAL

Supplemental material for this article may be found at http://mbio.asm.org /lookup/suppl/doi:10.1128/mBio.00034-11/-/DCSupplemental.

Figure S1, PDF file, 0.115 MB.
Figure S2, PDF file, 1.455 MB.
Table S1, XLS file, 0.106 MB.
Table S2, DOCX file, 0.024 MB.
Table S3, DOC file, 0.038 MB.

REFERENCES

1. **Jeong KS, Ahn J, Khodursky AB.** 2004. Spatial patterns of transcriptional activity in the chromosome of *Escherichia coli*. Genome Biol. **5**:R86.
2. **Peter BJ, et al.** 2004. Genomic transcriptional response to loss of chromosomal supercoiling in *Escherichia coli*. Genome Biol. **5**:R87.
3. **Blot N, Mavathur R, Geertz M, Travers A, Muskhelishvili G.** 2006. Homeostatic regulation of supercoiling sensitivity coordinates transcription of the bacterial genome. EMBO Rep. **7**:710–715.
4. **Balke VL, Gralla JD.** 1987. Changes in the linking number of supercoiled DNA accompany growth transitions in *Escherichia coli*. J. Bacteriol. **169**:4499–4506.
5. **Travers A, Muskhelishvili G.** 2005. Bacterial chromatin. Curr. Opin. Genet. Dev. **15**:507–514.
6. **Browning DF, Grainger DC, Busby SJW.** 2010. Effects of nucleoid-associated proteins on bacterial chromosome structure and gene expression. Curr. Opin. Microbiol. **13**:773–780.
7. **Dillon SC, Dorman CJ.** 2010. Bacterial nucleoid-associated proteins, nucleoid structure and gene expression. Nat. Rev. Microbiol. **8**:185–195.
8. **Rimsky S, Travers A.** 2011. Pervasive regulation of nucleoid structure and function by nucleoid-associated proteins. Curr. Opin. Microbiol. **14**:136–141.
9. **Malik M, Bensaid A, Rouviere-Yaniv J, Drlica K.** 1996. Histone-like protein HU and bacterial DNA topology: suppression of an HU deficiency by gyrase mutations. J. Mol. Biol. **256**:66–76.
10. **Schneider R, Travers A, Kutateladze T, Muskhelishvili G.** 1999. A DNA architectural protein couples cellular physiology and DNA topology in *Escherichia coli*. Mol. Microbiol. **34**:953–964.
11. **Travers A, Schneider R, Muskhelishvili G.** 2001. DNA supercoiling and transcription in *Escherichia coli*—the FIS connection. Biochimie **83**:213–217.
12. **Hatfield GW, Benham CJ.** 2002. DNA topology-mediated control of global gene expression in *Escherichia coli*. Annu. Rev. Genet. **36**:175–203.
13. **Keane OM, Dorman C.** 2003. The *gyr* genes of *Salmonella enterica* serovar

14. **Travers A, Muskhelishvili G.** 2005. DNA supercoiling—a global transcriptional regulator for enterobacterial growth? Nat. Rev. Microbiol. **3**:157–169.
15. **Cróinín TO, Dorman CJ.** 2007. Expression of the Fis protein is sustained in late-exponential- and stationary-phase cultures of *Salmonella enterica* serovar Typhimurium grown in the absence of aeration. Mol. Microbiol. **66**:237–251.
16. **Weinstein-Fischer D, Altuvia S.** 2007. Differential regulation of *Escherichia coli* topoisomerase I by Fis. Mol. Microbiol. **63**:1131–1144.
17. **Muskhelishvili G, Travers A.** 2009. Intrinsic *in vivo* modulators: negative supercoiling and the constituents of the bacterial nucleoid, p 69–95. In Buc H, Strick T (ed), RNA polymerases as molecular motors. RSC Publishing, Cambridge, United Kingdom.
18. **Berger M, et al.** 2010. Coordination of genomic structure and transcription by the main bacterial nucleoid-associated protein HU. EMBO Rep. **11**:59–64.
19. **Menzel R, Gellert M.** 1983. Regulation of the genes for E. coli DNA gyrase: homeostatic control of DNA supercoiling. Cell **34**:105–113.
20. **González-Gil G, Kahmann R, Muskhelishvili G.** 1998. Regulation of *crp* transcription by oscillation between distinct nucleoprotein complexes. EMBO J. **17**:2877–2885.
21. **Schneider R, Travers A, Muskhelishvili G.** 2000. The expression of the *Escherichia coli fis* gene is strongly dependent on the superhelical density of DNA. Mol. Microbiol. **38**:167–175.
22. **Hulton CS, et al.** 1990. Histone-like protein H1 (H-NS), DNA supercoiling, and gene expression in bacteria. Cell **63**:631–642.
23. **Drlica K.** 1992. Control of bacterial DNA supercoiling. Mol. Microbiol. **6**:425–433.
24. **Dorman CJ, Deighan P.** 2003. Regulation of gene expression by histone-like proteins in bacteria. Curr. Opin. Genet. Dev. **13**:179–184.
25. **Dame RT.** 2005. The role of nucleoid-associated proteins in the organization and compaction of bacterial chromatin. Mol. Microbiol. **56**:858–870.
26. **Deng S, Stein RA, Higgins NP.** 2005. Organization of supercoil domains and their reorganization by transcription. Mol. Microbiol. **57**:1511–1521.
27. **Hardy CD, Cozzarelli NR.** 2005. A genetic selection for supercoiling mutants of *Escherichia coli* reveals proteins implicated in chromosome structure. Mol. Microbiol. **57**:1636–1652.
28. **Kar S, et al.** 2006. Right-handed DNA supercoiling by an octameric form of histone-like protein HU: modulation of cellular transcription. J. Biol. Chem. **281**:40144–40153.
29. **Ogata Y, et al.** 1997. Heat shock-induced excessive relaxation of DNA in *Escherichia coli* mutants lacking the histone-like protein HU. Biochim. Biophys. Acta **1353**:298–306.
30. **Weinstein-Fischer D, Elgrably-Weiss M, Altuvia S.** 2000. *Escherichia coli* response to hydrogen peroxide: a role for DNA supercoiling, topoisomerase I and Fis. Mol. Microbiol. **35**:1413–1420.
31. **Kar S, Edgar R, Adhya S.** 2005. Nucleoid remodeling by an altered HU protein: reorganization of the transcription program. Proc. Natl. Acad. Sci. U. S. A. **102**:16397–16402.
32. **Marr C, Geertz M, Hütt MT, Muskhelishvili G.** 2008. Dissecting the logical types of network control in gene expression profiles. BMC Syst. Biol. **2**:18.
33. **Dorman CJ.** 1996. Flexible response: DNA supercoiling, transcription and bacterial adaptation to environmental stress. Trends Microbiol. **4**:214–216.
34. **Tse-Dinh YC, Qi H, Menzel R.** 1997. DNA supercoiling and bacterial adaptation: thermotolerance and thermoresistance. Trends Microbiol. **5**:323–326.
35. **Cheung KJ, Badarinarayana V, Selinger DW, Janse D, Church GM.** 2003. A microarray-based antibiotic screen identifies a regulatory role for supercoiling in the osmotic stress response of *Escherichia coli*. Genome Res. **13**:206–215.
36. **Sonnenschein N, Geertz M, Muskhelishvili G, Hütt M-T.** 2011. Analog regulation of metabolic demand. BMC Syst. Biol. **5**:40.
37. **Hsieh LS, Rouviere-Yaniv J, Drlica K.** 1991. Bacterial DNA supercoiling and ATP/ADP ratio: changes associated with salt shock. J. Bacteriol. **173**:3914–3917.
38. **van Workum M, et al.** 1996. DNA supercoiling depends on the phosphorylation potential in *Escherichia coli*. Mol. Microbiol. **20**:351–360.
39. **Snoep JL, van der Weijden CC, Andersen HW, Westerhoff HV, Jensen**

PR. 2002. DNA supercoiling in *Escherichia coli* is under tight and subtle homeostatic control, involving gene-expression and metabolic regulation of both topoisomerase I and DNA gyrase. Eur. J. Biochem. **269**: 1662–1669.

40. **Muskhelishvili G, Sobetzko P, Geertz M, Berger M.** 2010. General organisational principles of the transcriptional regulation system: a tree or a circle? Mol. Biosyst. **6**:662–676.

41. **Ishihama A.** 2000. Functional modulation of *Escherichia coli* RNA polymerase. Annu. Rev. Microbiol. **54**:499–518.

42. **Weber H, Polen T, Heuveling J, Wendisch VF, Hengge R.** 2005. Genome-wide analysis of the general stress response network in *Escherichia coli*: sigmaS-dependent genes, promoters, and sigma factor selectivity. J. Bacteriol. **187**:1591–1603.

43. **Hengge R.** 2009. Proteolysis of σ^S (RpoS) and the general stress response in *Escherichia coli*. Res. Microbiol. **160**:667–676.

44. **Kusano S, Ding Q, Fujita N, Ishihama A.** 1996. Promoter selectivity of *Escherichia coli* RNA polymerase Eσ70 and Eσ38 holoenzymes. Effect of DNA supercoiling. J. Biol. Chem. **271**:1998–2004.

45. **Bordes P, et al.** 2003. DNA supercoiling contributes to disconnect σ^S accumulation from σ^S-dependent transcription in *Escherichia coli*. Mol. Microbiol. **48**:561–571.

46. **Mukherjee K, Nagai H, Shimamoto N, Chatterji D.** 1999. GroEL is involved in activation of *Escherichia coli* RNA polymerase devoid of the ω subunit *in vivo*. Eur. J. Biochem. **266**:228–235.

47. **Minakhin L, et al.** 2001. Bacterial RNA polymerase subunit omega and eukaryotic RNA polymerase subunit RPB6 are sequence, structural, and functional homologs and promote RNA polymerase assembly. Proc. Natl. Acad. Sci. U. S. A. **98**:892–897.

48. **Typas A, Hengge R.** 2005. Differential ability of σ^S and σ70 of *Escherichia coli* to utilize promoters containing half or full UP-element sites. Mol. Microbiol. **55**:250–260.

49. **Salgado H, et al.** 2006. RegulonDB (version 5.0): *Escherichia coli* K-12 transcriptional regulatory network, operon organization, and growth conditions. Nucleic Acids Res. **34** (**database issue**):D394–D397.

50. **Liu LF, Wang JC.** 1987. Supercoiling of the DNA template during transcription. Proc. Natl. Acad. Sci. U. S. A. **84**:7024–7027.

51. **Cabrera JE, Cagliero C, Quan S, Squires CL, Jin DJ.** 2009. Active transcription of rRNA operons condenses the nucleoid in *Escherichia coli*: examining the effect of transcription on nucleoid structure in the absence of transertion. J. Bacteriol. **191**:4180–4185.

52. **Arnold GF, Tessman I.** 1988. Regulation of DNA superhelicity by *rpoB* mutations that suppress defective Rho-mediated transcription termination in *Escherichia coli*. J. Bacteriol. **170**:4266–4271.

53. **Drlica K, Franco RJ, Steck TR.** 1988. Rifampin and *rpoB* mutations can alter DNA supercoiling in *Escherichia coli*. J. Bacteriol. **170**:4983–4985.

54. **Typas A, Becker G, Hengge R.** 2007. The molecular basis of selective promoter activation by the σ^S subunit of RNA polymerase. Mol. Microbiol. **63**:1296–1306.

55. **Shin M, et al.** 2005. DNA looping-mediated repression by histone-like protein H–NS: specific requirement of Eσ70 as a cofactor for looping. Genes Dev **19**:2388–2398.

56. **Cheng B, Zhu C-X, Ji C, Ahumada A, Tse-Dinh Y-C.** 2003. Direct interaction between *Escherichia coli* RNA polymerase and the zinc ribbon domains of DNA topoisomerase. I. J. Biol. Chem. **278**:30705–30710.

57. **Gupta R, China A, Manjunatha UH, Ponnanna NM, Nagaraja V.** 2006. A complex of DNA gyrase and RNA polymerase fosters transcription in *Mycobacterium smegmatis*. Biochem. Biophys. Res. Commun. **4**:1141–1145.

58. **Hu P, et al.** 2009. Global functional atlas of *Escherichia coli* encompassing previously uncharacterized proteins. PLoS Biol. **7**:e96.

59. **Drolet M.** 2006. Growth inhibition mediated by excess negative supercoiling: the interplay between transcription elongation, R-loop formation and DNA topology. Mol. Microbiol. **59**:723–730.

60. **Jin DJ, Cabrera JE.** 2006. Coupling the distribution of RNA polymerase to global gene regulation and the dynamic structure of the bacterial nucleoid in *Escherichia coli*. J. Struct. Biol. **156**:284–291.

61. **Mathew R, Chatterji D.** 2006. The evolving story of the omega subunit of bacterial RNA polymerase. Trends Microbiol. **14**:450–455.

62. **Jishage M, Kvint K, Shingler V, Nyström T.** 2002. Regulation of sigma factor competition by the alarmone ppGpp. Genes Dev. **16**:1260–1270.

63. **Magnusson LU, Farewell A, Nyström T.** 2005. ppGpp: a global regulator in *Escherichia coli*. Trends Microbiol. **13**:236–242.

64. **Gentry DR, Xiao H, Burgess R, Cashel M.** 1991. The omega subunit of

65. **Chatterji D, Ogawa Y, Shimada T, Ishihama A.** 2007. The role of RNA polymerase omega subunit in expression of the *relA* gene in *Escherichia coli*. FEMS Microbiol. Lett. **267**:51–55.

66. **Vrentas CE, Gaal T, Ross W, Ebright RH, Gourse RL.** 2005. Response of RNA polymerase to ppGpp: requirement for the omega subunit and relief of this requirement by DksA. Genes Dev. **19**:2378–2387.

67. **Potrykus K, et al.** 2006. Antagonistic regulation of *Escherichia coli* ribosomal RNA *rrnB* P1 promoter activity by GreA and DksA. J. Biol. Chem. **22**:15238–15248.

68. **Magnusson LU, Gummesson B, Joksimovi P, Farewell A, Nyström T.** 2007. Identical, independent and opposing roles of ppGpp and DksA in *Escherichia coli*. J. Bacteriol. **189**:5193–5202.

69. **Gaal T, Mandel MJ, Silhavy TJ, Gourse RL.** 2006. Crl facilitates RNA polymerase holoenzyme formation. J. Bacteriol. **188**:7966–7970.

70. **Typas A, Barembruch C, Possling A, Hengge R.** 2007. Stationary phase reorganisation of the *Escherichia coli* transcription machinery by Crl protein, a fine-tuner of σS activity and levels. EMBO J. **26**:1569–1578.

71. **Flores N, et al.** 2008. New insights into the role of sigma factor RpoS revealed in *Escherichia coli* strains lacking the phosphoenolpyruvate: carbohydrate phosphotransferase system. J. Mol. Microbiol. Biotechnol. **14**:176–192.

72. **Colland F, Barth M, Hengge-Aronis R, Kolb A.** 2000. Sigma factor selectivity of Escherichia coli RNA polymerase: role for CRP, IHF and lrp transcription factors. EMBO J. **19**:3028–3037.

73. **Rochman M, Aviv M, Glaser G, Muskhelishvili G.** 2002. Promoter protection by a transcription factor acting as a local topological homeostat. EMBO Rep. **3**:355–360.

74. **Xu J, Johnson RC.** 1995. Identification of genes negatively regulated by Fis: Fis and RpoS comodulate growth-phase-dependent gene expression in *Escherichia coli*. J. Bacteriol. **177**:938–947.

75. **Gummesson B, et al.** 2009. Increased RNA polymerase availability directs resources towards growth at the expense of maintenance. EMBO J. **28**: 2209–2219.

76. **Zhou YN, Jin DJ.** 1998. The rpoB mutants destabilizing initiation complexes at stringently controlled promoters behave like "stringent" RNA polymerases in Escherichia coli. Proc. Natl. Acad. Sci. U. S. A. **95**: 2908–2913.

77. **Crozat E, Philippe N, Lenski RE, Geiselmann J, Schneider D.** 2005. Long-term experimental evolution in *Escherichia coli*. XII. DNA topology as a key target of selection. Genetics **169**:523–532.

78. **Magnusson LU, Nystrom T, Farewell A.** 2003. Underproduction of σ70 mimics a stringent response. A proteome approach. J. Biol. Chem. **278**: 968–973.

79. **Typas A, Hengge R.** 2006. Role of the spacer between the −35 and −10 regions in σS promoter selectivity in *Escherichia coli*. Mol. Microbiol. **59**: 1037–1051.

80. **Cairns BR.** 2009. The logic of chromatin architecture and remodeling at promoters. Nature **461**:193–198.

81. **Amann E, Brosius J.** 1985. ATG vectors for regulated high-level expression of cloned genes in *Escherichia coli*. Gene **40**:183–190.

82. **Schneider R, Travers A, Muskhelishvili G.** 1997. Fis modulates growth phase-dependent topological transitions of DNA in *Escherichia coli*. Mol. Microbiol. **26**:519–530.

83. **Sternbach H, Engelhardt R, Lezius AG.** 1975. Rapid isolation of highly active RNA polymerase from *Escherichia coli* and its subunits by matrix-bound heparin. Eur. J. Biochem. **60**:51–55.

84. **Hager DA, Jin DJ, Burgess RR.** 1990. Use of Mono Q high-resolution ion-exchange chromatography to obtain highly pure and active *Escherichia coli* RNA polymerase. Biochemistry **29**:7890–7894.

85. **Keller W.** 1975. Determination of the number of superhelical turns in simian virus 40 DNA by gel electrophoresis. Proc. Natl. Acad. Sci. U. S. A. **72**:4876–4880.

86. **Saeed AI, et al.** 2003. TM4: a free, open-source system for microarray data management and analysis. Biotechniques **34**:374–378.

87. **Cleveland W, Devlin S.** 1988. Locally weighted linear regression: an approach to regression analysis by local fitting. J. Am. Stat. Assoc. **83**: 596–609.

88. **Pan W.** 2002. A comparative review of statistical methods for discovering differentially expressed genes in replicated microarray experiments. Bioinformatics **18**:546–554.

Escherichia coli K-12 RNA polymerase is not required for stringent RNA control *in vivo*. J. Bacteriol. **12**:3901–3903.